



This information is current as of December 12, 2012.

## **A Phospholipase C- $\gamma$ 1-Independent, RasGRP1-ERK –Dependent Pathway Drives Lymphoproliferative Disease in Linker for Activation of T Cells–Y136F Mutant Mice**

Robert L. Kortum, Alexandre K. Rouquette-Jazdanian, Michihiko Miyaji, Robert K. Merrill, Evan Markegard, John M. Pinski, Amelia Wesselink, Nandan N. Nath, Clayton P. Alexander, Wenmei Li, Noemi Kedei, Jeroen P. Roose, Peter M. Blumberg, Lawrence E. Samelson and Connie L. Sommers

*J Immunol* published online 3 December 2012  
<http://www.jimmunol.org/content/early/2012/12/02/jimmunol.1201458>

---

**Supplementary Material** <http://www.jimmunol.org/content/suppl/2012/12/03/jimmunol.1201458.DC1.html>

**Subscriptions** Information about subscribing to *The Journal of Immunology* is online at: <http://jimmunol.org/subscriptions>

**Permissions** Submit copyright permission requests at: <http://www.aai.org/ji/copyright.html>

**Email Alerts** Receive free email-alerts when new articles cite this article. Sign up at: <http://jimmunol.org/cgi/alerts/etoc>



# A Phospholipase C- $\gamma$ 1-Independent, RasGRP1-ERK-Dependent Pathway Drives Lymphoproliferative Disease in Linker for Activation of T Cells-Y136F Mutant Mice

Robert L. Kortum,\* Alexandre K. Rouquette-Jazdanian,\* Michihiko Miyaji,\*<sup>1</sup>  
 Robert K. Merrill,\* Evan Markegard,<sup>†</sup> John M. Pinski,\* Amelia Wesselink,\*  
 Nandan N. Nath,\* Clayton P. Alexander,\* Wenmei Li,\* Noemi Kedei,<sup>‡</sup> Jeroen P. Roose,<sup>†</sup>  
 Peter M. Blumberg,<sup>‡</sup> Lawrence E. Samelson,\* and Connie L. Sommers\*

Mice expressing a germline mutation in the phospholipase C- $\gamma$ 1-binding site of linker for activation of T cells (LAT) show progressive lymphoproliferation and ultimately die at 4–6 mo age. The hyperactivated T cells in these mice show defective TCR-induced calcium flux but enhanced Ras/ERK activation, which is critical for disease progression. Despite the loss of LAT-dependent phospholipase C- $\gamma$ 1 binding and activation, genetic analysis revealed RasGRP1, and not Sos1 or Sos2, to be the major Ras guanine exchange factor responsible for ERK activation and the lymphoproliferative phenotype in these mice. Analysis of isolated CD4<sup>+</sup> T cells from LAT-Y136F mice showed altered proximal TCR-dependent kinase signaling, which activated a Zap70- and LAT-independent pathway. Moreover, LAT-Y136F T cells showed ERK activation that was dependent on Lck and/or Fyn, protein kinase C- $\theta$ , and RasGRP1. These data demonstrate a novel route to Ras activation in vivo in a pathological setting. *The Journal of Immunology*, 2013, 190: 000–000.

Engagement of the TCR by a peptide/MHC complex ligand triggers tyrosine phosphorylation of ITAMs on the TCR $\zeta$  and CD3 chains by the Src family kinases (SFKs) Lck and Fyn, allowing for the recruitment and activation of the tyrosine kinase ZAP70 (1). ZAP70 then rapidly phosphorylates the membrane-bound adaptor linker for activation of T cells (LAT) on five of nine conserved tyrosines in its C-terminal tail, four of which (Y136, Y175, Y195, Y235) seem critical for the adaptor function of LAT (2). These phosphorylated tyrosines then act as docking sites for SH2 domain-containing proteins, allowing for the recruitment of numerous multiprotein complexes to LAT. Recruitment of these signaling complexes to the membrane by LAT activates multiple intracellular signaling pathways controlling both T cell development and effector functions (3).

Activation of the small G protein Ras is central to numerous physiologic and pathologic conditions. In T cells, phosphorylated LAT associates with two molecular complexes that regulate Ras activation: phospholipase C (PLC)- $\gamma$ 1/GADS/SLP-76 and Grb2/Sos (4). PLC- $\gamma$ 1 interacts with LAT p-Y136, and stabilization of this interaction by the adaptors GADS (binds LAT p-Y175 and p-Y195) and SLP-76 (binds GADS and PLC- $\gamma$ 1) allows for phosphorylation of PLC- $\gamma$ 1 on residues critical for its activation (5). Activated PLC- $\gamma$ 1 then cleaves phosphatidylinositol 4,5-bisphosphate, generating inositol 1,4,5-triphosphate, which stimulates release of intracellular calcium stores, and diacylglycerol (DAG). DAG activates the Ras guanine exchange factor (RasGEF) RasGRP1 both directly by binding its C1 domain and indirectly by activating novel protein kinase C (PKC) isoforms, which phosphorylate RasGRP1 on T184 and increases its RasGEF activity (6).

The RasGEFs Sos1 and Sos2 are constitutively associated with the adaptor Grb2 and are recruited to the membrane where they have basal RasGEF activity via Grb2/LAT interactions (Grb2 binds LAT p-Y175, p-Y195, and p-Y235) (5). Furthermore, Sos proteins contain an allosteric Ras-GTP binding site that, when engaged, markedly enhances their RasGEF activity (7). Ras-GTP binding to Sos allows for the engagement of a positive feedback loop between Ras and Sos, primed by either RasGRP1 or basal Sos activity, which can be employed when high levels of Ras activation are required (8, 9). Generation of activated Ras then activates multiple downstream pathways, including the Raf/MEK/ERK kinase cascade, to drive both T cell development and effector functions (10, 11).

Studies assessing the role of LAT in vivo using mouse models have revealed that LAT is essential for T cell development. LAT deletion or a knock-in mutation of the distal 4 tyrosine residues of LAT (LAT-4YF) led to a complete block in pre-TCR-driven developmental signals and failure of T cell precursors to develop beyond the CD4<sup>-</sup>CD8<sup>-</sup> (double-negative [DN]) stage (12, 13). Knock-in mutations of either Y175/195/235F (3YF) or Y136F (1YF) in LAT caused a DN thymocyte block in young mice (14–16).

\*Laboratory of Cellular and Molecular Biology, National Cancer Institute, National Institutes of Health, Bethesda, MD 20892; <sup>†</sup>Department of Anatomy, University of California San Francisco, San Francisco, CA 94143; and <sup>‡</sup>Laboratory of Cancer Biology and Genetics, National Cancer Institute, National Institutes of Health, Bethesda, MD 20892

<sup>1</sup>Current address: First Department of Internal Medicine, Kansai Medical University, Osaka, Japan.

Received for publication May 25, 2012. Accepted for publication November 2, 2012.

This work was supported by the Intramural Research Program of the Center for Cancer Research, National Cancer Institute, National Institutes of Health. R.L.K. received additional support from a Pharmacology Research and Training Fellowship, National Institute of General Medical Sciences, National Institutes of Health.

Address correspondence and reprint requests to Connie L. Sommers, Laboratory of Cellular and Molecular Biology and Center for Cancer Research, National Cancer Institute, National Institutes of Health, 37 Convent Drive, Building 37, Room 2064, Bethesda, MD 20892-4256. E-mail address: sommersc@helix.nih.gov

The online version of this article contains supplemental material.

Abbreviations used in this article: DAG, diacylglycerol; DKO, double-knockout; DN, double-negative; DP, double-positive; IP, immunoprecipitation; LAT, linker for activation of T cells; LN, lymph node; NP-40, Nonidet P-40; pc-PLC, phosphatidylcholine-specific phospholipase C; PKC, protein kinase C; PLC, phospholipase C; PLD, phospholipase D; RasGEF, Ras guanine exchange factor; Ras-PD, Ras-GTP pull-down; SFK, Src family kinase; WCL, whole-cell lysate; WT, wild-type.

However, as these mice aged they developed a marked postthymic expansion of either  $\gamma\delta$  or  $\alpha\beta$  T cells, respectively (14–16), leading to massive splenomegaly, lymph node enlargement, and lymphocyte infiltration of nonlymphoid organs. The hyperproliferative  $\alpha\beta$  T cells found in LAT-Y136F mice show a Th2 CD4<sup>+</sup> activated/memory phenotype (CD44<sup>hi</sup>CD62L<sup>lo</sup>) indicative of prior stimulation (14, 16), and they require signals from both MHC class II and CD28 for their development (17). Isolated CD4<sup>+</sup> T cells from LAT-Y136F mice showed defective TCR-dependent PLC- $\gamma$ 1 phosphorylation and Ca<sup>2+</sup> flux (16) consistent with the mutation of the Y136 PLC- $\gamma$ 1-binding site on LAT. However, these mutant CD4<sup>+</sup> T cells showed a hyperactivation of ERK kinase signaling that helped drive disease progression (18). Genetic analysis showed that this altered ERK activation was dependent, in part, on a novel Bam32-ERK signaling pathway, as Bam32 deletion led to a reduction in ERK signaling and delayed disease progression in LAT-Y136F mice (18).

We sought to further characterize the altered signaling pathways that drive ERK hyperactivation, pathologic lymphocyte proliferation, and disease progression in LAT-Y136F mice. We found that the small G protein Ras was hyperactivated in CD4<sup>+</sup> T cells from LAT-Y136F mice. However, despite lacking PLC- $\gamma$ 1 activation, genetic analysis showed that disease progression and ERK signaling were more dependent on RasGRP1 than on Sos1/2 in LAT-Y136F mice. Analysis of upstream signaling in T cells from these mice revealed Lck and Fyn hyperactivation that did not signal through ZAP70, but activated an unconventional SFK/PKC $\theta$ /RasGRP1 pathway to contribute to ERK signaling and disease in this murine model of pathologic lymphocyte proliferation.

## Materials and Methods

### Mice

RasGRP1<sup>-/-</sup> mice were a gift from James Stone (University of Alberta, Edmonton, AB, Canada) (19). Sos2<sup>-/-</sup> mice were generated at the Laboratory of Cellular and Molecular Biology by Eugene Santos (University of Salamanca, Salamanca, Spain) (20). Lck-Cre (21) mice were purchased from Taconic. T cell-specific deletion of Sos1 (denoted Sos1(T)<sup>-/-</sup>) was achieved by crossing Sos1<sup>fl/fl</sup> mice to mice expressing Lck-Cre (22). Genotyping for LAT-Y136F (16), RasGRP1<sup>-/-</sup> (19), Sos1(T)<sup>-/-</sup> (22), Sos2<sup>-/-</sup> (20), and Cre (21) mice was carried out as detailed in the original publications. All mice were housed at the National Institutes of Health following guidelines set forth by the National Cancer Institute–Bethesda Animal Care and Use Committee.

### Flow cytometry

Single-cell suspensions from thymus or pooled axillary, brachial, and inguinal lymph nodes were stained with the fluorochrome-conjugated mAbs described in the text. Flow cytometry was performed using a FACSCalibur and CellQuest software (BD Biosciences), and data were analyzed using FlowJo software (Tree Star). All fluorochrome-conjugated Abs were purchased from BD Biosciences.

### Cell purification

For CD4<sup>+</sup> lymph node (LN) T cells, total lymphocytes were isolated using a CD4<sup>+</sup> T cell isolation kit (Miltenyi Biotec) according to the manufacturer's instructions. Cells were >90% CD4<sup>+</sup> following purification. Purified CD4<sup>+</sup> LN cells were then resuspended in prewarmed RPMI 1640 at 1 × 10<sup>6</sup> cells/10  $\mu$ l and allowed to equilibrate to room temperature for 20 min before any additional manipulation.

### Cell stimulation, immunoprecipitation, Ras pull-down, and Western blotting

For stimulation of purified CD4<sup>+</sup> lymphocytes, purified cells were resuspended in prewarmed RPMI 1640 at 1 × 10<sup>6</sup> cells/10  $\mu$ l. For each time point, 4 × 10<sup>6</sup> cells were preincubated with 10  $\mu$ g/ml biotinylated anti-CD3e (145-2C11; BD Biosciences) with or without 10  $\mu$ g/ml biotinylated anti-CD4 (GK1.5; BD Biosciences) for 15 min at room temperature. For inhibitor studies, cells were pretreated for 20 min with

inhibitor in RPMI 1640 prior to incubation with stimulatory Abs. The inhibitors used included: pan-SFK inhibitor PP2 (23) at 20  $\mu$ M (Sigma-Aldrich), classical PKC inhibitor Gö6976 (24) at 5  $\mu$ M (Sigma-Aldrich), pan-PKC inhibitor Gö6983 (25) at 5  $\mu$ M (Sigma-Aldrich), PKC inhibitor rottlerin (26) at 20  $\mu$ M (Sigma-Aldrich), PLC- $\gamma$ 1 inhibitor U73122 (27, 28) at 1  $\mu$ M (Sigma-Aldrich), inactive enantiomer U73343 (27) at 1  $\mu$ M (Sigma-Aldrich), phospholipase D (PLD) and phosphatidylcholine-specific PLC (pc-PLC) inhibitor D609 (29) at 300  $\mu$ M (Alexis Biochemicals), or MEK1/2 inhibitor U0126 (30) at 10  $\mu$ M (Cell Signaling Technology). All inhibitors were dissolved in DMSO, with a final DMSO concentration of <2.5% v/v in RPMI 1640. Cells were then washed with RPMI 1640 and resuspended at 1 × 10<sup>6</sup> cells/10  $\mu$ l prior to the addition of 40  $\mu$ l 2× streptavidin (20  $\mu$ g/ml final concentration). Stimulation was terminated by the addition of 2× SDS sample buffer containing 100 mM DTT and boiling for 10 min.

For immunoprecipitations (IPs) and Ras-GTP pull-downs (Ras-PDs), 5 × 10<sup>6</sup> (phospho-pan Src [Y416] IPs) or 10 × 10<sup>6</sup> (Ras-PDs, TCR $\zeta$  IPs, Lck IPs, and PCK $\theta$  IPs) cells were stimulated as described above or were stimulated without CD4 costimulation (Lck and PCK $\theta$  IPs). For IPs, samples were lysed for 10 min in ice-cold Nonidet P-40 (NP-40) lysis buffer (1% NP-40, 10% glycerol, 150 mM NaCl, 50 mM Tris [pH 7.5], 1 mM sodium vanadate, protease inhibitor mixture; Roche) and precleared using protein A/G agarose (Santa Cruz Biotechnology). Lysates were then immunoprecipitated using anti-phospho-pan Src Y416 (1:50; Cell Signaling Technology) or anti-PCK $\theta$  (sc-212, 1:100; Santa Cruz Biotechnology) for 1 h. IPs were washed four times in ice-cold lysis buffer without inhibitors. For Ras pull-downs, cells were lysed on ice for 10 min in Ras-PD lysis buffer (1% NP-40, 50 mM Tris [pH 7.5], 200 mM NaCl, 2.5 mM MgCl<sub>2</sub>, 1 mM PMSF, protease inhibitor mixture; Roche) and spun at 10,000 rpm for 10 min. GST fused with the Ras binding domain of Raf-1 bound to glutathione-Sepharose beads was prepared as previously described (31) and used to isolate Ras-GTP from lysates by rotating incubation for 1 h at 4°C. Samples were washed four times in Ras-PD lysis buffer. All samples were boiled in 2× SDS sample buffer containing 100 mM DTT for 10 min prior to Western blotting.

Samples were loaded at 0.5 × 10<sup>6</sup> cells per lane and separated by 10% SDS-PAGE. The following primary Abs were used: pMEK1/2 (1:1000; Cell Signaling Technology no. 9154), MEK1/2 (1:1000 each; BD Transduction Laboratories no. 610122 [MEK1] and no. 610236 [MEK2]), pERK1/2 (1:2000; Cell Signaling Technology no. 4370), ERK1/2 (1:2000; Cell Signaling Technology no. 4695), Ras (1:1000; Upstate Biotechnology no. 05-516),  $\beta$ -actin (1:5000; Sigma-Aldrich no. AC-40), pPKC $\theta$  (T538) (1:2000; Cell Signaling Technology no. 9377), PKC $\theta$  (1:500; Santa Cruz Biotechnology no. sc-212), PKC $\delta$  (1:2000; Santa Cruz Biotechnology no. sc-937), pRasGRP1 T184 (1:2000; see below), RasGRP1 (1:500; Santa Cruz Biotechnology no. sc-8430), phospho-tyrosine 4G10 (1:4000; Millipore no. 05-321), phospho-pan Src (1:2000; Cell Signaling Technology [Y416] no. 2101), Lck (1:2000; Cell Signaling Technology no. 2752), Fyn (1:1000 each; Santa Cruz Biotechnology no. sc-365913 and no. sc-73388), Yes (1:1000; Santa Cruz Biotechnology no. sc-46674), pZAP70 (1:2000; Cell Signaling Technology no. 2704), ZAP70 (1:2000) (32) and TCR $\zeta$  (1:1000) (33). Blots were incubated with primary Ab at 4°C overnight and secondary HRP (1:20,000; Millipore) Abs at room temperature for 1 h. ECL was used to visualize protein products (SuperSignal West Pico and SuperSignal West Femto; Pierce). Protein bands were quantified using ImageJ. Anti-pRasGRP1 T184 mouse mAb was generated by immunization with the peptide SRKL-pT-QRIKSNTC by Eurogentech/AnaSpec (Fremont, CA). The column-purified Ab was used at 1:2000 in 5% BSA. Western blots of phosphorylated proteins were stripped and reprobed for their total proteins with the exception of pMEK1/2 and total MEK1/2, as the harsh conditions required to strip the pMEK blots removed the associated MEK proteins as well. For these blots, parallel gels were equally loaded and run simultaneously.

### Subcellular fractionation

Subcellular fractionation was performed as previously described (34). Briefly, cells were washed once in ice-cold PBS and resuspended in a hypotonic lysis buffer (10 mM Tris-HCl [pH 7.5], 5 mM MgCl<sub>2</sub>, 1 mM EGTA, 100  $\mu$ M NaVO<sub>4</sub>). Cells were then passed 30 times through a 25-gauge needle and incubated on ice for 10 min, and nuclei and unlysed cells were removed by centrifugation at 300 × g for 5 min. Postnuclear supernatants were then spun at 100,000 × g for 60 min and separated into the soluble (S100) and insoluble (P100) fractions. P100 fractions were resuspended using equal volumes of 2× SDS sample buffer. S100 and P100 fractions were probed with LAT and GAPDH Abs to ensure >95% enrichment of each fraction (data not shown).

### Statistical analysis

All data are presented as averages  $\pm$  SD. The significance of the difference between means of two data sets was determined by a two-tailed Student *t* test. A *p* value  $<0.05$  was considered statistically significant. Linear regression analyses of spleen weight data were performed using GraphPad Prism software. For pairwise comparisons, the slopes of regression analysis were analyzed for differences in disease progression (Supplemental Table I). A *p* value  $<0.05$  was considered statistically significant.

### Results

Mice carrying a germline mutation in the PLC- $\gamma$ 1-binding site of LAT (LAT-Y136F) exhibit a pathologic CD4<sup>+</sup> T cell lymphoproliferation dependent on the ERK signaling cascade, in part mediated by the adaptor molecule Bam32 (18). We sought to further characterize the signaling pathways that led to lymphoproliferative disease and ERK activation in these mice. Assessment of Ras activation in isolated CD4<sup>+</sup> T cells from LAT-Y136F mice showed increased basal Ras-GTP levels, which were modestly increased by mild plate-bound anti-CD3 $\epsilon$  stimulation, but markedly enhanced by PMA stimulation (Fig. 1A). To assess whether these pathologic cells show an enhanced capacity to activate Ras, CD4<sup>+</sup> T cells isolated from wild-type (WT) or LAT-Y136F mice were rested for 6 h to normalize basal Ras-GTP levels prior to stimulation with PMA with or without ionomycin. CD4<sup>+</sup> T cells from LAT-Y136F mice showed a marked increase in PMA-stimulated Ras-GTP levels compared with WT controls (Fig. 1B). These data led us to hypothesize that the lymphoproliferative disease observed in LAT-Y136F mice (14, 16) was, at least partially, dependent on hyperactivation of Ras.

#### *Sos1/2* deletion slows lymphoproliferative disease progression in LAT-Y136F mice

Once phosphorylated, LAT normally associates with two regulators of Ras activation: PLC- $\gamma$ 1, which activates the RasGEF RasGRP1 via DAG, and Grb2, which directly associates with the RasGEFs Sos1 and Sos2 (4). The combined actions of RasGRP1, Sos1, and Sos2 are thought to induce complete Ras activation downstream of the TCR (6, 8, 9, 35). Because TCR-induced LAT-PLC- $\gamma$ 1 association and activation should be abrogated in LAT-Y136F mice (14, 16), we thought that it would be unlikely that RasGRP1 would be activated, and rather that the Ras hyperactivation in LAT-Y136F mice was due to signaling through Sos1 and/or Sos2.

To directly test this hypothesis, LAT-Y136F mice were crossed to *Sos1*(T)<sup>-/-</sup> and/or *Sos2*<sup>-/-</sup> mice (11, 20, 22) to assess the development of lymphoproliferative disease in the absence of these RasGEFs (Figs. 2, 3). Deletion of *Sos1* or *Sos2* alone did not affect the lymphoproliferative disease seen in LAT-Y136F mice as assessed by a time-dependent increase in spleen weight (Fig. 2). Furthermore, assessment of lymph nodes from LAT-Y136F mice by staining with anti-CD4 and anti-CD8 Abs followed by flow cytometry showed a CD4<sup>+</sup> T lymphocyte accumulation, which was not altered by *Sos1* or *Sos2* deletion (Fig. 3). In contrast, combined *Sos1/2* deletion significantly slowed LAT-Y136F disease progression, as assessed by either a change in the slope of the regression curve for the time-dependent increases in spleen weight (Fig. 2A, Supplemental Table I) or the accumulation of CD4<sup>+</sup> lymphocytes (Fig. 3A).

LAT-Y136F mice show a substantial early block (DN to double-positive [DP]) in thymocyte development (14, 16), and we have previously shown that *Sos1* is similarly required for thymocyte development at the DN-to-DP transition (11, 22). Based on these data, one could hypothesize that the reduction in disease burden seen in *Sos1/2* double-knockout (DKO) mice could simply be due to delayed thymic development and thus a reduced development

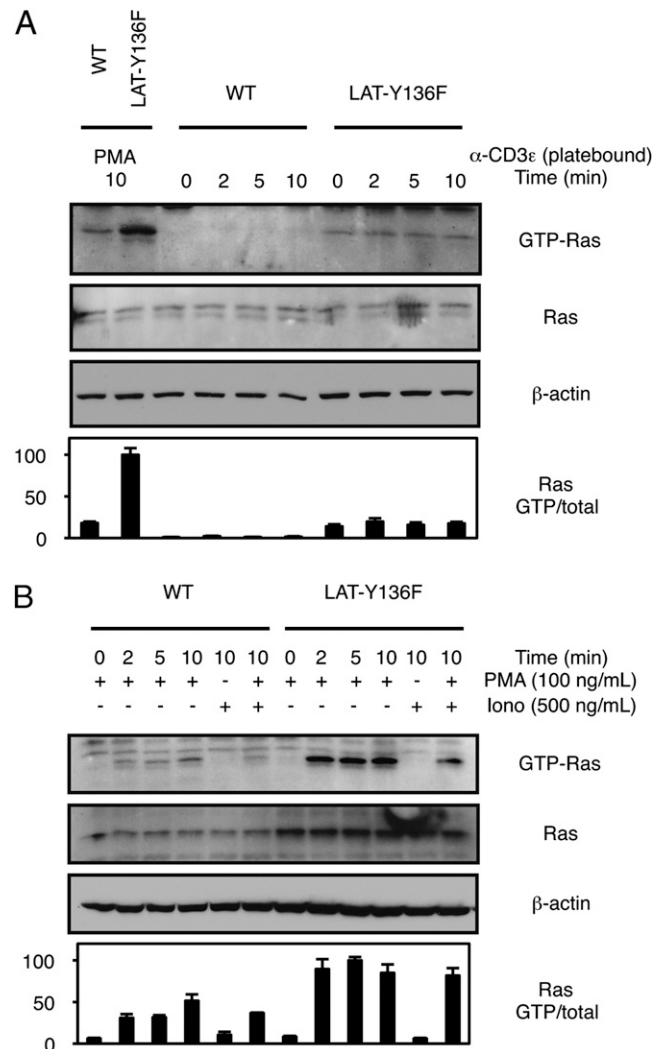


**FIGURE 1.** CD4<sup>+</sup> T cells isolated from LAT-Y136F mice show elevated Ras activation. (A and B) Western blotting (above, quantified below) for activated Ras from a GST-Ras binding domain pull-down (top) or for total Ras or  $\beta$ -actin in WCL from purified CD4<sup>+</sup> LN cells from WT versus LAT-Y136F mice stimulated with (A) either 100 ng/ml PMA for 10 min or 5  $\mu$ g/ml plate-bound anti-CD3 $\epsilon$  Ab for the indicated times or (B) 100 ng/ml PMA with or without 500 ng/ml ionomycin for the indicated times. Data are representative of two independent experiments.

of CD4<sup>+</sup> T lymphocytes. To determine whether *Sos1* and/or *Sos2* deletion altered thymocyte development in LAT-Y136F mice, thymi from young (4-wk-old) mice were analyzed to examine thymocyte development at a point where pathologic CD4<sup>+</sup> T cells are beginning to appear but have not yet overwhelmed the animals (14, 16). Staining with anti-CD4 and anti-CD8 to assess thymocyte development revealed a marked block at the DN-to-DP transition in LAT-Y136F mice (Fig. 4A), with a marked decrease in the number of CD4<sup>+</sup>CD8<sup>+</sup> (DP) thymocytes (Fig. 4B) and an increase in the DN/DP ratio (Fig. 4C). Whereas combined *Sos1/2* deletion was required to delay lymphoproliferative disease in LAT-Y136F mice (Figs. 2, 3), deletion of either *Sos1* alone or in combination with *Sos2* enhanced the DN-to-DP developmental block seen in thymi of young LAT-Y136F mice as assessed by a decrease in the number of DP thymocytes (Fig. 4B) and an increase in the DN/DP ratio (Fig. 4A, 4C). Because either *Sos1* deletion (which did not affect LAT-Y136F lymphoproliferative disease) or combined *Sos1/2* deletion (which did delay LAT-Y136F lymphoproliferative disease) showed the same block in

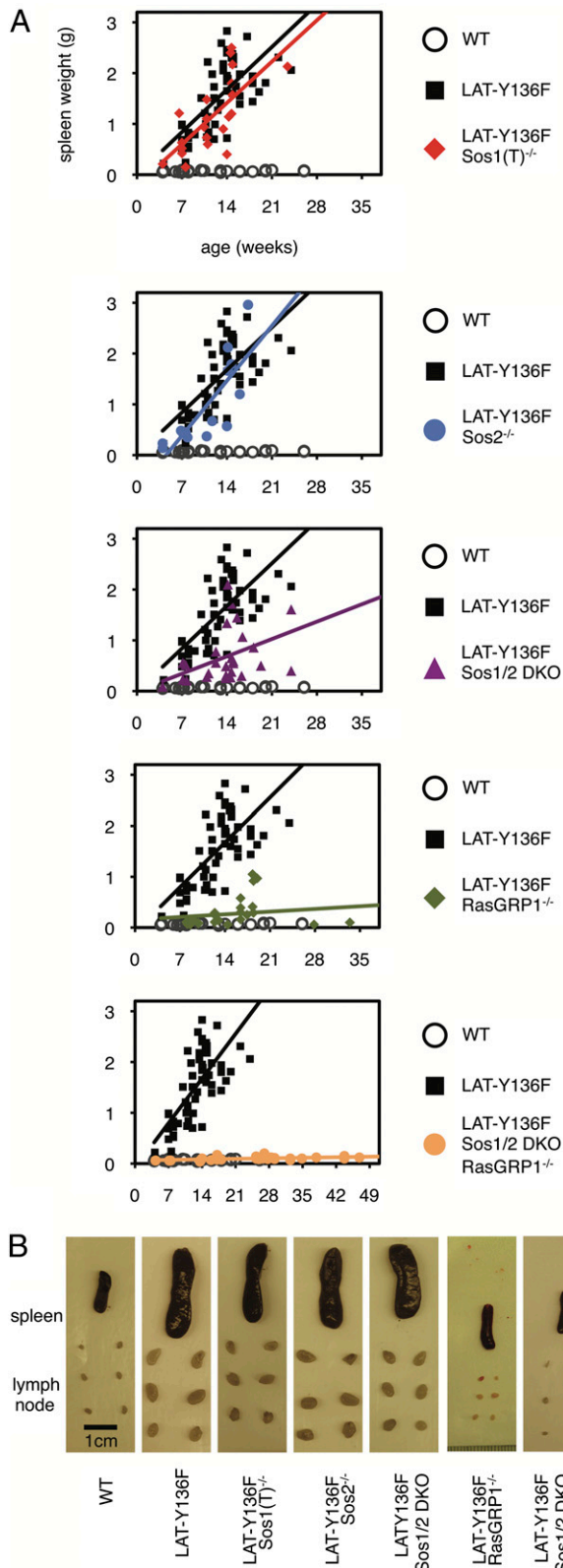


**FIGURE 2.** RasGRP1, and not *Sos1/2*, is the major RasGEF responsible for splenomegaly in LAT-Y136F mice. **(A)** Quantification of spleen weight versus time from WT mice, LAT-Y136F mice, LAT-Y136F mice deleted for *Sos1* and/or *Sos2*, or LAT-Y136F mice deleted for RasGRP1 and/or *Sos1/2*. Each symbol represents one mouse. Data were accumulated over time from several experiments, and the same accumulated data from WT and LAT-Y136F mice are shown in each graph as controls to compare the LAT-Y136F/RasGEF crosses. LAT-Y136F/*Sos1/2* DKO, LAT-Y136F/*RasGRP1*<sup>-/-</sup>, and LAT-Y136F/*Sos1/2* DKO/*RasGRP1*<sup>-/-</sup> mice showed

thymocyte development, these data show that delaying thymic development alone is insufficient to reduce the disease burden in LAT-Y136F mice.

We next examined whether *Sos1/2* deletion directly affected Raf/MEK/ERK kinase cascade activation in CD4<sup>+</sup> T lymphocytes isolated from LAT-Y136F mice. Combined *Sos1/2* deletion diminished, but did not eliminate, both basal and anti-CD3e- plus anti-CD4-stimulated MEK and ERK phosphorylation in LAT-Y136F mice (Fig. 5A). These data suggest that although signaling through *Sos1/2* contributes to ERK activation in this disease model, other *Sos1/2*-independent signaling pathways contribute to disease progression in LAT-Y136F mice.

#### *RasGRP1* is the major RasGEF responsible for Ras/ERK activation and lymphoproliferative disease in LAT-Y136F mice

Because *Sos1/2* deletion did not eliminate ERK hyperactivation and disease progression in LAT-Y136F mice, we addressed the role of RasGRP1 by crossing LAT-Y136F mice to *RasGRP1*<sup>-/-</sup> mice (Figs. 2, 3). Unexpectedly, RasGRP1 deletion led to a major reduction in disease progression compared with LAT-Y136F mice when assessing both the time-dependent increase in spleen weight (Fig. 2) and CD4<sup>+</sup> lymphocyte accumulation (Fig. 3) seen in LAT-Y136F mice. Direct comparison of LAT-Y136F/*Sos1/2* DKO versus LAT-Y136F/*RasGRP1*<sup>-/-</sup> mice showed significant differences in CD4<sup>+</sup> lymphocyte accumulation (Fig. 3A), but the rates of disease progression (Fig. 2A) between these two groups were not quite statistically different ( $p = 0.07$ ; Supplemental Table I). These data suggest that deletion of either *Sos1/2* or RasGRP1 has a statistically similar effect on the rate of lymphoproliferation in LAT-Y136F mice. Combined deletion of *Sos1/2* and RasGRP1 in LAT-Y136F mice (LAT-Y136F/*Sos1/2* DKO/*RasGRP1*<sup>-/-</sup> mice) eliminated lymphoproliferative disease such that 15 mice examined at >27 wk age remained disease free (Figs. 2, 3). LAT-Y136F/*Sos1/2* DKO/*RasGRP1*<sup>-/-</sup> mice showed a rate of disease progression that was statistically different from LAT-Y136F/*Sos1/2* DKO mice, but not LAT-Y136F/*RasGRP1*<sup>-/-</sup> mice (Supplemental Table I). These data suggest that RasGRP1 deletion has a more profound effect than *Sos1/2* deletion on disease progression in LAT-Y136F mice (Fig. 2A). Furthermore, RasGRP1 deletion almost completely eliminated both basal and anti-CD3e-plus anti-CD4-stimulated MEK and ERK phosphorylation in T cells from LAT-Y136F mice (Fig. 5B). These data suggest that a RasGRP1-dependent, PLC- $\gamma$ 1-independent pathway is the major determinant driving both proliferation and ERK activation in LAT-Y136F mice.

#### An SFK- and PKC-dependent pathway lies upstream of RasGRP1 in CD4<sup>+</sup> T lymphocytes isolated from LAT-Y136F mice

We next sought to determine which altered upstream signaling pathways were leading to PLC- $\gamma$ 1-independent RasGRP1 activation. Phosphotyrosine blotting of whole-cell lysates (WCL) from anti-CD3e plus anti-CD4-stimulated LAT-Y136F CD4<sup>+</sup> T lymphocytes showed a decrease in tyrosine-phosphorylated

significant differences in the slope of the regression line ( $p < 0.05$ ) from LAT-Y136F, LAT-Y136F/*Sos1*<sup>-/-</sup>, or LAT-Y136F/*Sos2*<sup>-/-</sup> mice, indicating a significant slowing of disease progression upon deletion of *Sos1/2* and/or RasGRP1. In contrast, a similar rate in disease progression was noted when comparing LAT-Y136F/*Sos1/2* DKO to LAT-Y136F/*RasGRP1*<sup>-/-</sup> mice. A complete statistical analysis of the data is given in Supplemental Table I. **(B)** Images of spleen (above) and isolated axillary, brachial, and inguinal lymph nodes (below) from 7-wk-old mice indicated in (A).

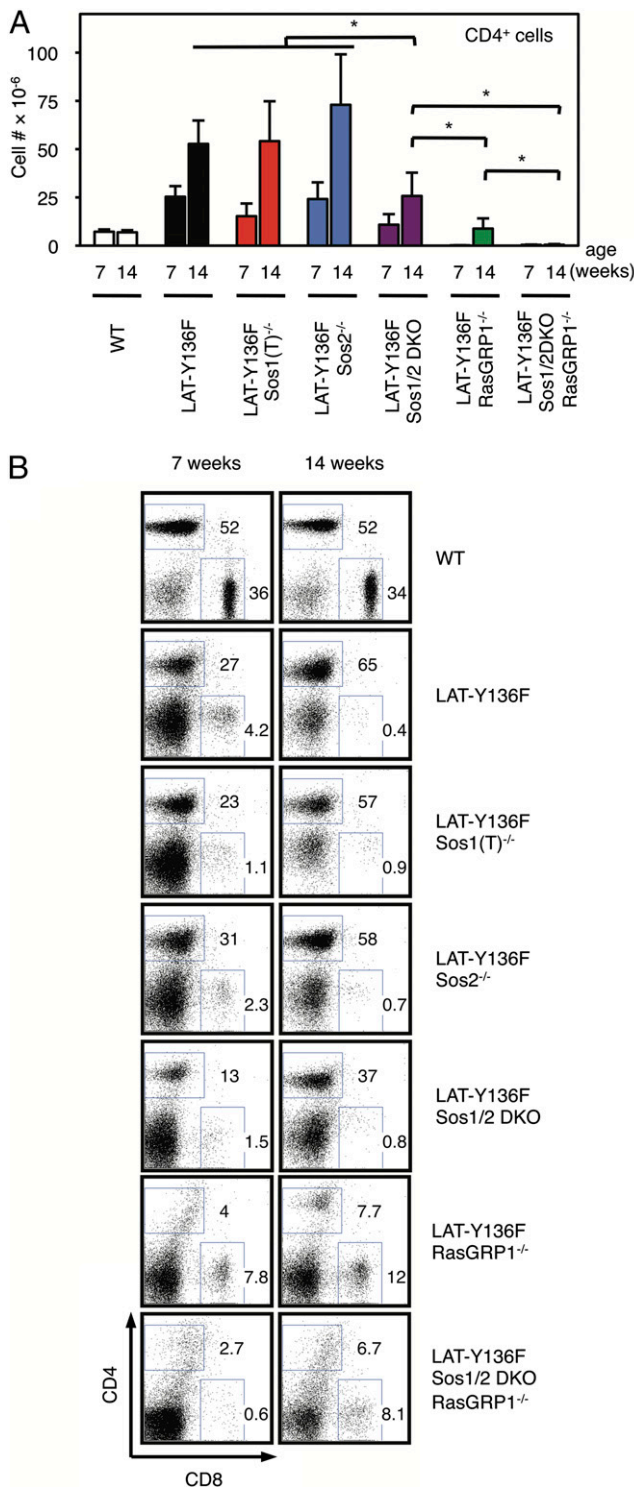


**FIGURE 3.** RasGRP1, and not Sos1/2, is the major RasGEF responsible for lymphoproliferation in LAT-Y136F mice. (A) Quantification of CD4<sup>+</sup> LN T cell numbers from pooled axillary, brachial, and inguinal lymph nodes stained with anti-CD4 and anti-CD8 from 7- or 14-wk-old mice indicated in Fig. 2 ( $n \geq 4$  for each group). Data are represented as means  $\pm$  SD. \* $p < 0.05$ . (B) Flow cytometry dot plots of pooled axillary, brachial, and inguinal lymph nodes stained with anti-CD4 and anti-CD8 from mice indicated in (A).

proteins at 38, 70, and 76 kDa (consistent with LAT, ZAP70, and SLP-76; small arrowheads) compared with WT CD4<sup>+</sup> T lymphocytes (Fig. 6A). However, we observed a significant increase in both basal

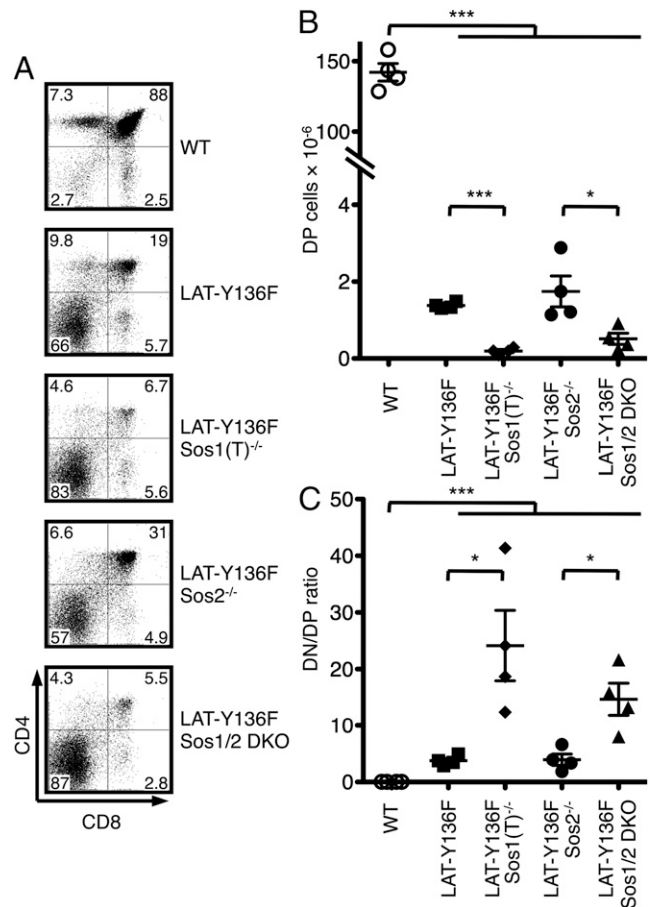


**FIGURE 4.** Sos1-dependent pre-TCR developmental block does not correlate with delayed disease in LAT-Y136F mice. (A) Flow cytometry dot plots of thymocytes stained with anti-CD4 and anti-CD8 from 4-wk-old WT mice, LAT-Y136F mice, or LAT-Y136F mice deleted for Sos1 and/or Sos2 ( $n = 4$  for each group). (B) Total numbers of DP thymocytes isolated from 4-wk-old mice from (A) ( $n = 4$  for each). Each symbol denotes an individual mouse and the bar denotes the average for the group. (C) The DN/DP ratio from (A). \* $p < 0.05$ , \*\*\* $p < 0.001$ .

and stimulated phosphorylation of a doublet at 55 kDa (consistent with phosphorylated SFKs; Fig. 6A, large arrowhead). All SFKs contain distinct tyrosine residues that, when phosphorylated, are either activating or inhibitory. In Src, these residues are Y416 and Y505, respectively, and the Abs targeting these sites recognize all SFKs. Probing with phospho-specific Abs for the active (pY416) and inactive (pY505) forms of SFKs revealed a marked enhancement in tyrosine phosphorylation at the activating site and a decrease in phosphorylation at the inhibitory site (Fig. 6B), indicating a marked increase in the activation state of SFKs in LAT-Y136F CD4<sup>+</sup> T cells.

This SFK activation could have been due to either an enhanced activation of SFKs normally expressed in T cells (Lck, Fyn, and Yes) or aberrant expression and activation of SFKs not normally expressed to a significant degree in T lymphocytes (Src, Fgr, Hck, Blk, and Fyn). Immunoprecipitation for the activated form of the SFKs (pY416) followed by blotting for total individual SFKs revealed that Lck, Fyn, and, to a lesser extent, Yes, but not other SFKs, were hyperactivated in LAT-Y136F CD4<sup>+</sup> T lymphocytes (Fig. 6C and data not shown). Furthermore, RasGRP1 deletion did not diminish the high levels of SFK phosphorylation seen in LAT-Y136F CD4<sup>+</sup> T lymphocytes, suggesting that SFK hyperactivation was upstream of RasGRP1 (Fig. 6D).

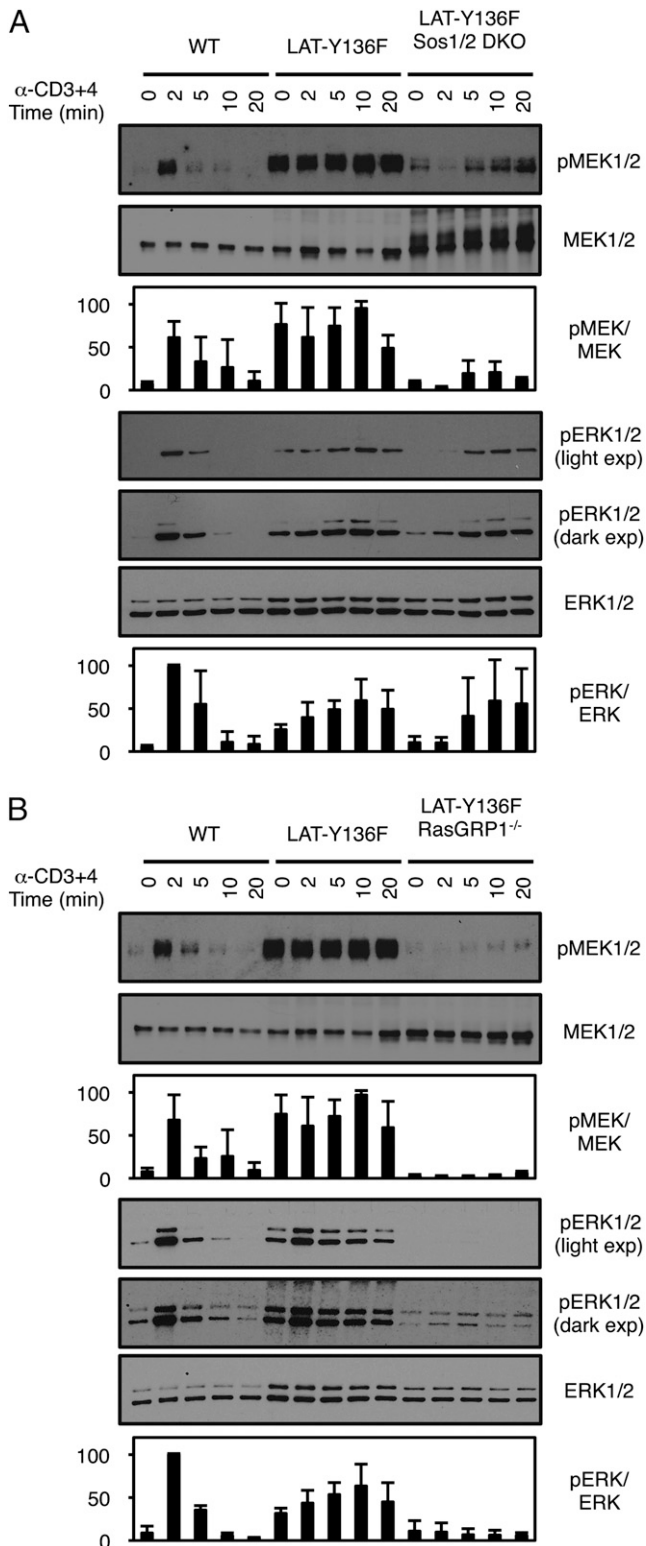


**FIGURE 5.** RasGRP1 is the major RasGEF responsible for ERK activation in T cells from LAT-Y136F mice. (**A** and **B**) Western blotting (above, quantified below) for phospho-MEK, total MEK, phospho-ERK, or total ERK in WCL from purified CD4<sup>+</sup> LN cells from WT, LAT-Y136F, or LAT-Y136F mice crossed to *Sos1/2* DKO mice (**A**) or *RasGRP1*<sup>-/-</sup> mice (**B**) stimulated with 10 μg/ml soluble anti-CD3ε plus anti-CD4 Abs. All stimulations were for the indicated times in minutes. Total MEK blots were loaded in parallel and run at the same time as pMEK blots. Data are representative of three independent experiments.

Downstream of TCR/MHC engagement, activated SFKs Lck and Fyn normally phosphorylate ITAM domains on the TCRζ and CD3 chains, leading to recruitment and activation of the tyrosine kinase ZAP70 (1). However, LAT-Y136F CD4<sup>+</sup> T cells have an activated phenotype (CD44<sup>hi</sup>CD62L<sup>lo</sup>CD45RB<sup>lo</sup>TCRβ<sup>lo</sup>; Refs. 14, 16) and show low surface TCR/CD3 complex expression compatible with activation-induced TCR downregulation (Refs. 14, 16 and Fig. 6E). Phosphorylation of TCRζ, the major docking site for ZAP70 on the TCR/CD3 complex, was dramatically decreased in LAT-Y136F CD4<sup>+</sup> T lymphocytes (Fig. 6E), possibly due to low levels of TCRζ surface expression. Furthermore, the high level of active SFK observed in LAT-Y136F CD4<sup>+</sup> T cells was uncoupled from ZAP70, as both phosphorylation of ZAP70 at its active site (Fig. 6B and Ref. 17) and coimmunoprecipitation between Lck and ZAP70 (Fig. 7A) were actually decreased in CD4<sup>+</sup> T cells from LAT-Y136F mice compared with WT controls.

Because high levels of SFK activity did not lead to elevated ZAP70 phosphorylation, it seemed unlikely that “canonical” signaling pathways were contributing to the elevated, RasGRP1-dependent, basal ERK activation observed in LAT-Y136F CD4<sup>+</sup> T cells (Fig. 5). We therefore sought to determine whether the elevated SFK signals were shunted to RasGRP1 via normal, alternative signaling pathways. Previous studies have shown that PKCθ can associate with and be activated by the SFK Lck (36–38). We observed enhanced basal coimmunoprecipitation between Lck and PKCθ in CD4<sup>+</sup> T cells isolated from LAT-Y136F mice (Fig. 7A, 7B). This interaction was specific, as Lck did not coimmunoprecipitate to a detectable level with the closely related PKC family member PKCδ (Fig. 7A).

PKCθ membrane recruitment, which depends on association of its C1 domain with DAG (39, 40), is enhanced by its association with and activation by Lck (41). We therefore tested whether LAT-Y136F CD4<sup>+</sup> T cells showed enhanced PKCθ membrane recruitment (Fig. 7C) and activation (Fig. 7D). PKCθ levels were elevated in crude membrane extracts (P100 fractions) isolated from LAT-Y136F CD4<sup>+</sup> T cells compared with WT controls (Fig. 7C), indicating that DAG-dependent recruitment of PKCθ is elevated in LAT-Y136F CD4<sup>+</sup> T cells. Immunoblotting for an activating site (T538) in the activation loop of PKCθ showed enhanced basal phosphorylation of PKCθ in CD4<sup>+</sup> T cells isolated from LAT-Y136F mice (Fig. 7D). These data suggest that the elevated SFK activity observed in LAT-Y136F CD4<sup>+</sup> T cells could directly signal to PKCθ, leading to elevated PKCθ activation and downstream signaling.

RasGRP1 is a direct target of PKCθ, and activation of RasGRP1 depends on both its DAG-dependent recruitment to the membrane and on its phosphorylation by PKCθ on T184 (6). RasGRP1 levels were elevated basally in crude membrane extracts (P100 fractions) isolated from LAT-Y136F CD4<sup>+</sup> T cells compared with WT controls (Fig. 7C), indicating that its DAG-dependent recruitment is enhanced in LAT-Y136F CD4<sup>+</sup> T cells. To assess PKCθ-dependent phosphorylation of RasGRP1, we generated a phospho-specific Ab specific to T184, the site on RasGRP1 phosphorylated by PKCθ (Supplemental Fig. 1). Similar to PKCθ, phosphorylation of RasGRP1 on T184 was enhanced in LAT-Y136F CD4<sup>+</sup> T cells (Fig. 7D). These data (Figs. 6, 7) are consistent with signals from both activated SFKs and PKCθ emanating to RasGRP1 and ERK in LAT-Y136F CD4<sup>+</sup> T cells.

To help determine whether the ERK hyperactivation seen in LAT-Y136F CD4<sup>+</sup> T lymphocytes was downstream of both the SFKs and PKC, CD4<sup>+</sup> T lymphocytes isolated from either WT or LAT-Y136F mice were pretreated with inhibitors of these kinases prior to stimulation with anti-CD3ε plus anti-CD4. The SFK inhibitor PP2 (23) efficiently inhibited ERK activation (both basal

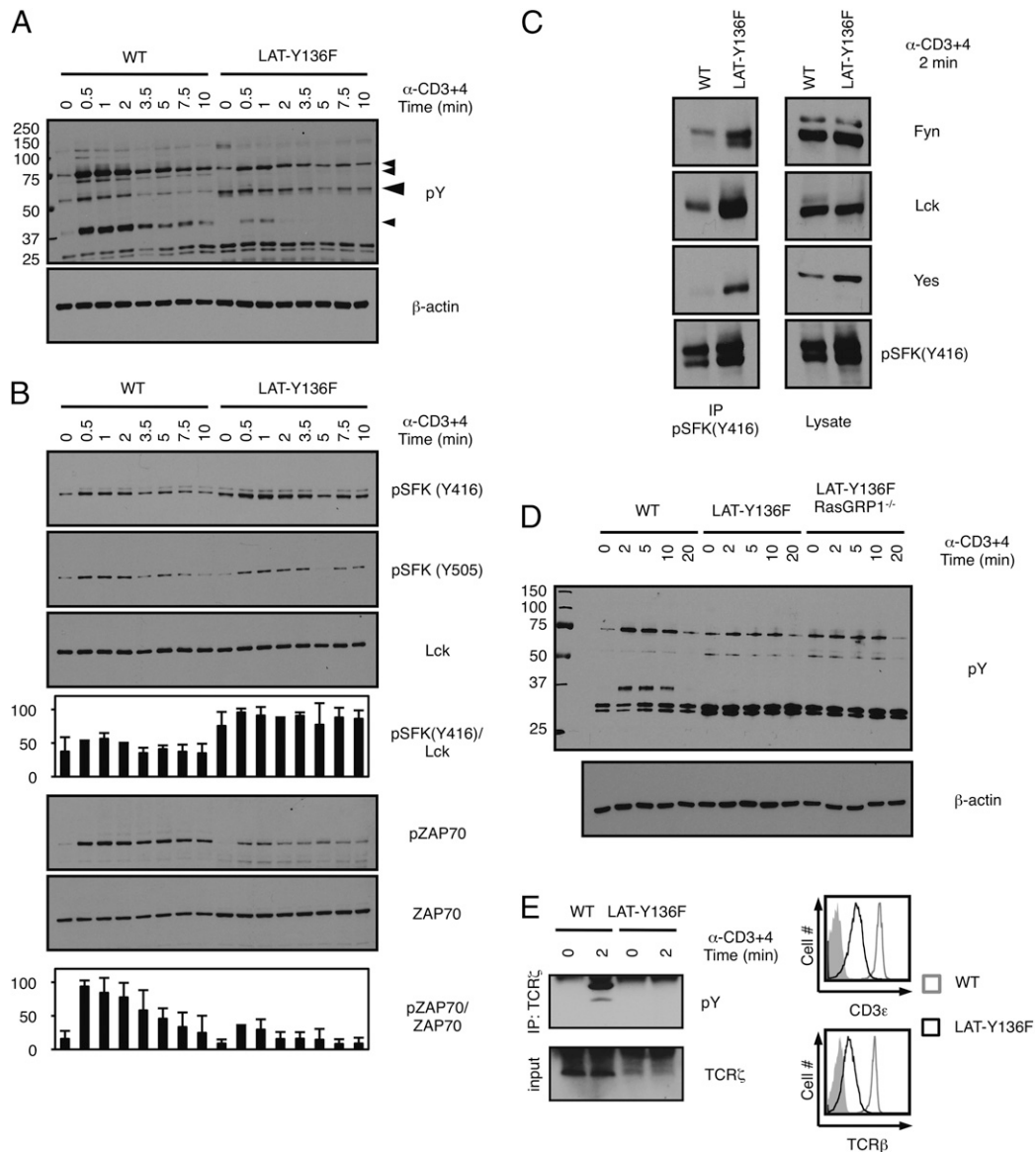


**FIGURE 6.** Altered activation of upstream kinases in T cells from LAT-Y136F mice. **(A and B)** Western blotting for phospho-tyrosine (4G10) and  $\beta$ -actin (A) or for active phospho-pan Src (Y416), inactive phospho-pan Src (Y505), total Lck, phospho-ZAP70, and total ZAP70 (*above*, quantified *below*) (B) in WCL from purified CD4<sup>+</sup> LN cells from WT and LAT-Y136F mice stimulated with 10  $\mu$ g/ml soluble anti-CD3e plus anti-CD4 Abs for the indicated times in minutes. On the phospho-tyrosine blot, small arrowheads represent putative SLP-76, ZAP70, and LAT bands and the large arrowhead represents a putative SFK doublet as outlined in the text. Data are representative of two independent experiments. **(C)** Western blotting for Lck, Fyn, Yes, and phospho-pan Src (Y416) in anti-phospho-pan Src (Y416) immunoprecipitates (*left*) or WCL (*right*) from purified CD4<sup>+</sup> LN cells from WT and LAT-Y136F mice stimulated with 10  $\mu$ g/ml soluble anti-CD3e plus anti-CD4 Abs for 2 min. Data are representative of two independent experiments. **(D)** Western blotting for phospho-tyrosine (4G10) and  $\beta$ -actin in WCL from purified CD4<sup>+</sup> LN cells from WT, LAT-Y136F, and LAT-Y136F/RasGRP1<sup>-/-</sup> mice stimulated with 10  $\mu$ g/ml soluble anti-CD3e plus anti-CD4 Abs for the indicated times in minutes. Data are representative of three independent experiments. **(E)** Western blotting for pY and TCR $\zeta$  in TCR $\zeta$  IPs from purified CD4<sup>+</sup> LN cells from either WT or LAT-Y136F mice stimulated with 10  $\mu$ g/ml soluble anti-CD3e Abs for the indicated times in minutes. Representative data are from two independent experiments (*left*), and histogram of anti-CD3e (*above*) or anti-TCR $\beta$  (*below*) staining in gated, CD4<sup>+</sup> lymphocytes from 8-wk-old WT versus LAT-Y136F mice is shown.

and stimulated) in both WT and LAT-Y136F CD4<sup>+</sup> T lymphocytes, indicating that ERK was downstream of SFKs in LAT-Y136F T cells (Fig. 8A, 8B). We next examined whether PKC $\theta$  was required for ERK hyperactivation in LAT-Y136F mice. The PKC family of enzymes can be divided into three branches based on their activation requirements: conventional (DAG- and Ca<sup>2+</sup>-dependent), novel (DAG-dependent but Ca<sup>2+</sup>-independent), and atypical (DAG- and Ca<sup>2+</sup>-independent). To examine PKC $\theta$  activation (a novel PKC family member), a combination of inhibitors to either conventional or total (pan-isoform) PKC enzymes was used. The total PKC inhibitor Gö6983 (25) and rottlerin, which has been reported to

inhibit the novel PKCs  $\delta$  (26) and  $\theta$  (42), reduced ERK activation to a much greater extent than did the conventional PKC inhibitor Gö6976 (24) (Fig. 8A), supporting the hypothesis that signaling from PKC $\theta$  or another novel PKC drives ERK hyperactivation in T cells from LAT-Y136F mice.

PKC $\theta$  activation is normally facilitated by PLC- $\gamma$ 1-dependent DAG production. However, whereas inhibition of PLC- $\gamma$ 1 using U73122 (27, 28) efficiently inhibited ERK activation in CD4<sup>+</sup> T lymphocytes isolated from WT mice (Fig. 8B), it did not alter the ERK hyperactivation observed in LAT-Y136F T cells (Fig. 8A), confirming the PLC- $\gamma$ 1-independent nature of this altered

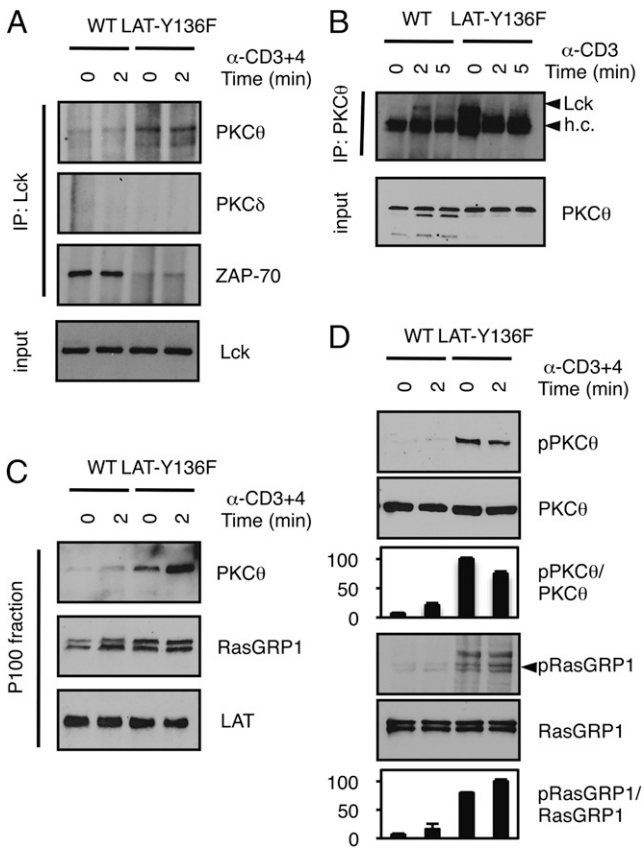


**FIGURE 7.** Enhanced Lck/PKC $\theta$  association and RasGRP1 membrane localization in CD4<sup>+</sup> T lymphocytes isolated from LAT-Y136F mice. **(A)** Western blotting for PKC $\theta$ , PKC $\delta$ , and ZAP70 in Lck IPs and total Lck in WCL from purified CD4<sup>+</sup> LN cells from either WT or LAT-Y136F mice stimulated with 10  $\mu$ g/ml soluble anti-CD3 $\epsilon$  Abs for the indicated times in minutes. Data are representative of three independent experiments. **(B)** Western blotting for Lck in PKC $\theta$  IPs and total PKC $\theta$  in WCL from purified CD4<sup>+</sup> LN cells from either WT or LAT-Y136F mice stimulated with 10  $\mu$ g/ml soluble anti-CD3 $\epsilon$  Abs for the indicated times in minutes. Data are representative of three independent experiments. **(C)** Western blotting for PKC $\theta$ , RasGRP1, and LAT in membrane (P100) fractions from purified CD4<sup>+</sup> LN cells from either WT or LAT-Y136F mice stimulated with 10  $\mu$ g/ml soluble anti-CD3 $\epsilon$  Abs for the indicated times in minutes. Data are representative of two independent experiments. **(D)** Western blotting for pPKC $\theta$  (T538), total PKC $\theta$ , pRasGRP1 (T184, doublet denoted by arrow), and total RasGRP1 (*above*, quantified *below*) in WCL from purified CD4<sup>+</sup> LN cells from either WT or LAT-Y136F mice stimulated with 10  $\mu$ g/ml soluble anti-CD3 $\epsilon$  plus anti-CD4 Abs for the indicated times in minutes. Data are representative of four independent experiments. h.c., Ig H chain.

signaling pathway. U73343, an inactive enantiomer of U73122, was used as a control and showed no effect in either WT or LAT-Y136F CD4<sup>+</sup> T cells. We also tested whether pc-PLC and/or PLD (other phospholipases that contribute to DAG production) substituted for PLC- $\gamma$ 1 in LAT-Y136F T cells by using the pc-PLC and PLD inhibitor D609 (29). Whereas D609 partially reduced anti-CD3 $\epsilon$ - plus anti-CD4-stimulated ERK activation in both WT and LAT-Y136F CD4<sup>+</sup> T cells (Fig. 8A, 8B), D609 significantly inhibited basal ERK activation in LAT-Y136F CD4<sup>+</sup> T cells (Fig. 8A). These data suggest that alternative sources of DAG cooperate with Lck/PKC $\theta$  signaling to drive RasGRP1 membrane localization (Fig. 7C) and activation (Fig. 7D), leading to basal ERK hyperactivation in T cells from LAT-Y136F mice.

Although these data suggest a linear pathway from Lck to RasGRP1 via activation of PKC $\theta$ , it still remained formally possible that SFK and PKC $\theta$  promote ERK activation independently

of RasGRP1. To assess the epistatic nature of SFK, PKC $\theta$ , and RasGRP1 signaling to ERK, CD4<sup>+</sup> T cells from LAT-Y136F were isolated and pretreated with either SFK (PP2) or PKC (Gö6983 [total PKC] and rottlerin [PKC $\theta$ - and PKC $\delta$ -specific]) inhibitors followed by Western blotting for phosphorylated PKC $\theta$  and RasGRP1. SFK inhibition significantly inhibited both PKC $\theta$  and RasGRP1 phosphorylation, suggesting that SFKs are upstream of both PKC $\theta$  and RasGRP1, whereas PKC inhibition reduced RasGRP1 phosphorylation, suggesting that PKC $\theta$  is upstream of RasGRP1 in LAT-Y136F CD4<sup>+</sup> T cells (Fig. 8C). These data suggest a linear signaling sequence emanating from Lck, through PKC $\theta$ , to RasGRP1 that drives ERK hyperactivation and disease in LAT-Y136F CD4<sup>+</sup> mice.

## Discussion

Mice encoding a germline mutation in the PLC- $\gamma$ 1-binding site of LAT (LAT-Y136F mice) (14, 16) develop an overwhelming Th2 CD4<sup>+</sup> T cell lymphoproliferation that is dependent on the ERK signaling cascade (18). Dissection of signaling pathways upstream of ERK revealed Ras hyperactivation in LAT-Y136F T cells. Ras is activated downstream of the TCR by the combined actions of the RasGEFs RasGRP1, Sos1, and Sos2. RasGRP1 activation normally depends on PLC- $\gamma$ 1-dependent generation of DAG, which acts both directly on RasGRP1 and indirectly by activating PKC $\theta$ , which can phosphorylate and enhance RasGRP1 activity (6). Sos1/2 activation depends both on Grb2-dependent recruitment to LAT and on binding to activated Ras-GTP to enhance Sos catalytic activity (7, 9). We have previously defined a Bam32-dependent pathway in LAT-Y136F mice. LAT-Y136F/Bam32<sup>-/-</sup> mice show a decrease in ERK activation that correlates with the extent of disease progression (18). However, in that study it was apparent that the Bam32-dependent pathway was not the exclusive determinant of disease. Based on a loss of PLC- $\gamma$ 1 activation (16, 17), we had originally hypothesized that the Bam32-independent signaling to ERK seen in LAT-Y136F mice would be Sos1/2-dependent. Therefore, we assessed whether Sos1/2 or RasGRP1 deletion could alter the lymphoproliferative phenotype in LAT-Y136F mice.

Surprisingly, RasGRP1 deletion had a more pronounced effect on both ERK1/2 phosphorylation (Fig. 5) and lymphoproliferative disease in LAT-Y136F mice (Figs. 2, 3) than did Sos1/2 deletion. However, comparison of the effects of Sos1/2 and RasGRP1 in animal models are complicated by both their combined requirements during lymphocyte development (11) and their reported interdependence during TCR signaling (9). We have previously reported that the combined actions of Sos1 and RasGRP1 are required for pre-TCR-driven proliferation beyond the DN3 checkpoint (11, 22). Furthermore, RasGRP1<sup>-/-</sup> mice show a significant block in positive selection (19). Therefore, developmental effects caused by these knockout models, in conjunction with the developmental effects caused by the LAT-Y136F mutation (16, 43), can complicate interpretation of alterations in the disease state of the animals. Using Sos1(T)<sup>-/-</sup> and Sos1/2 DKO mice (which have identical effects on thymocyte development when crossed to a LAT-Y136F background; Fig. 4), we found that indeed Sos1/2 DKO altered LAT-Y136F lymphoproliferative disease independent of altering thymocyte development.

It remained unclear, however, whether the effect of Sos1/2 deletion was a direct consequence of LAT/Grb2-mediated Sos1/2 activation or of the presence of a RasGRP1/Ras/Sos/Ras-positive feedback loop (8, 9). When assessing the effects of Sos1/2 and RasGRP1 deletion, each RasGEF knockout independently delayed disease progression in LAT-Y136F mice (Supplemental Table I). Comparison between these two groups showed

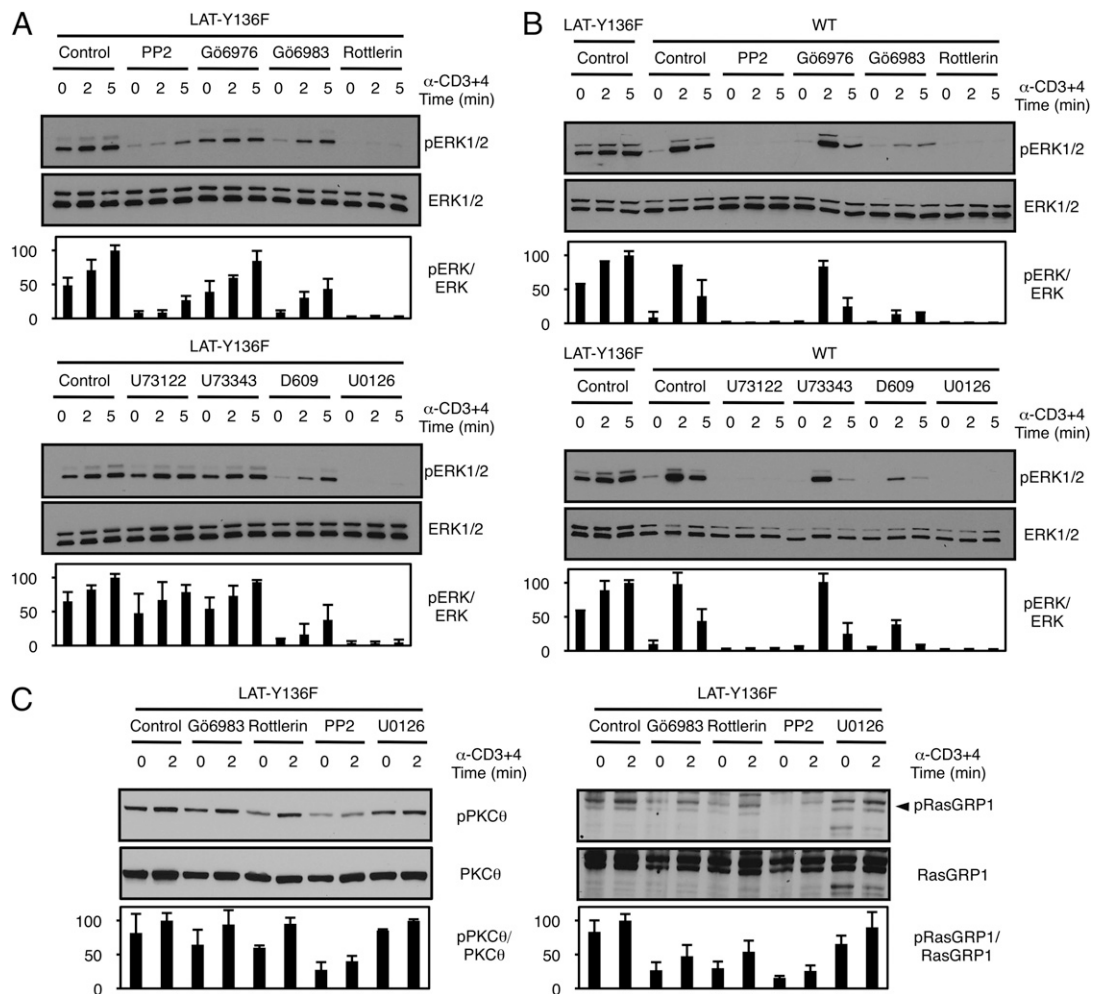


**FIGURE 8.** SFK and novel PKC signaling are required for ERK hyperactivation in CD4<sup>+</sup> T lymphocytes isolated from LAT-Y136F mice. (**A** and **B**) Western blotting for phospho-ERK and total ERK (*above*, quantified *below*) in WCL from purified CD4<sup>+</sup> LN cells from either LAT-Y136F (**A**) or WT (**B**) mice. Lysates were pretreated with the indicated inhibitors and then stimulated with 10  $\mu$ g/ml soluble anti-CD3 $\epsilon$  plus anti-CD4 Abs. DMSO-treated cells represent the vehicle control, and MEK1/2 inhibition by U0126 is the positive control showing a complete loss of ERK phosphorylation. All stimulations were for the indicated times in minutes. Data are representative of three independent experiments. (**C**) Western blotting for pPKC $\theta$  (T538), total PKC $\theta$ , pRasGRP1 (T184, doublet denoted by arrow), and total RasGRP1 (*above*, quantified *below*) in WCL from purified CD4<sup>+</sup> LN cells from LAT-Y136F mice. Lysates were pretreated with the indicated inhibitors and then stimulated with 10  $\mu$ g/ml soluble anti-CD3 $\epsilon$  plus anti-CD4 Abs. DMSO-treated cells represent the vehicle control. All stimulations were for the indicated times in minutes. Data are representative of two independent experiments.

less CD4<sup>+</sup> lymphocyte accumulation in LAT-Y136F/RasGRP1<sup>-/-</sup> mice than in LAT-Y136F/Sos1/2 DKO mice (Fig. 3A). These data are compatible with RasGRP1 being dominant to Sos1/2, with the contribution of Sos1/2 limited to a potential RasGRP1/Ras/Sos-positive feedback loop. However, effects on disease progression between these two groups were not statistically different ( $p = 0.07$ ; Fig. 2A). Because these two groups may have similar rates of disease progression (Fig. 2A, Supplemental Table I) but differences in accumulated disease at a given time (7 and 14 wk; Fig. 3A), we cannot rule out the possibility that some of differences observed between RasGRP1 and Sos1/2 deletion are due to developmental effects owing to RasGRP1 deficiency.

We observed a complete loss of lymphoproliferative disease in LAT-Y136F/RasGRP1<sup>-/-</sup>/Sos1/2 DKO mice, suggesting that Sos1/2 cannot be completely downstream of RasGRP1, otherwise the LAT-Y136F/RasGRP1<sup>-/-</sup> and LAT-Y136F/Sos1/2 DKO/RasGRP1<sup>-/-</sup> phenotypes would be identical. However, the rate of disease progression in LAT-Y136F/Sos1/2 DKO/RasGRP1<sup>-/-</sup> mice was different from LAT-Y136F/Sos1/2 DKO mice, but not from LAT-Y136F/RasGRP1<sup>-/-</sup> mice. These data suggest that RasGRP1 is the dominant RasGEF driving the disease phenotype.

A complete understanding of the interplay between Sos1/2 and RasGRP1 and how the RasGEF-dependent pathways are tied into Bam32-dependent signaling in LAT-Y136F mice will require combined RasGRP1/Bam32 and/or Sos1/2/Bam32 deletion on a LAT-Y136F background.

We (16, 18, 43) and others (14, 17, 44) simultaneously generated and described LAT-Y136F mice. However, whereas the overall phenotypes of these mice are strikingly similar, dissection of the molecular mechanisms that drive disease initiation and progression have yielded divergent conclusions. When examining TCR (anti-CD3- plus anti-CD4-induced) signaling in LAT-Y136F CD4<sup>+</sup> T cells, both laboratories have reported defective or absent LAT phosphorylation, PLC- $\gamma$ 1 phosphorylation, and Ca<sup>2+</sup> flux (16, 17), whereas examination of ERK activation has yielded differing results. We observe ERK hyperactivation (18) whereas Malissen and colleagues (17) do not see ERK activation in LAT-Y136F CD4<sup>+</sup> T cells. Although we do not understand the difference observed between the two laboratories, one possibility relates to our finding that the timing of the signaling experiments after dissection is critical. Our signaling experiments have revealed that whereas freshly isolated LAT-Y136F CD4<sup>+</sup> T lymphocytes show

high basal activation of SFK/Ras/ERK signaling, significant resting of cells after isolation can either reduce this basal ERK signaling (after 5 h) (Ref. 18 and data not shown) or eliminate differences in ERK activation from WT mice (after overnight culture) (16).

By examining upstream signaling in freshly isolated cells, we found basal and TCR-stimulated SFK hyperactivation in LAT-Y136F CD4<sup>+</sup> T cells (Fig. 6). Although we still do not fully understand the origin of SFK hyperactivation in LAT-Y136F mice, we hypothesize that the unique signaling environment caused by the marked TCR/CD3 complex downregulation seen in LAT-Y136F CD4<sup>+</sup> T cells (Fig. 6E and Refs. 14, 16) underlies many of the signaling anomalies. In LAT-Y136F CD4<sup>+</sup> T cells, there is very low/undetectable TCR $\zeta$  phosphorylation (Fig. 6E), an adaptation likely responsible for the decrease in ZAP70 docking and activation. This reduced TCR $\zeta$  phosphorylation may account for the inefficiency in Lck/ZAP70 interaction (Fig. 7A) and ZAP70 phosphorylation (Fig. 6B) seen in LAT-Y136F CD4<sup>+</sup> T cells.

The loss of canonical ZAP70 signaling could potentially modify activity of one of several regulatory axes controlling SFK activity, for example Csk-CD45 signaling (45, 46), Shp-1/ERK signaling (47), or signaling through the E3 ubiquitin ligase Cbl (48). Alternatively, feedback regulation of ZAP70 by the adaptor and LAT binding partner SLP-76 has been reported, with both ZAP70 phosphorylation and clustering being inhibited in SLP-76-deficient Jurkat cells (49, 50). Furthermore, it has been suggested that LAT itself is a negative regulator of T cell signaling by an unknown mechanism (51). However, whether SLP-76 and/or LAT truly exhibit a level of feedback regulation on SFK remains to be seen.

We therefore sought to determine whether the elevated SFK signals were shunted to RasGRP1 via alternative signaling pathways and identified an SFK/PKC $\theta$ /RasGRP1 signaling pathway that became dominant in the altered signaling environment created by the LAT-Y136F mutation. There exists significant precedence for the existence of SFK-dependent, ZAP70- and LAT-independent signaling in T cells. First, studies using ZAP70-deficient Jurkat cells have shown SFK- and PKC-dependent, ZAP70-independent ERK activation (52). Second, previous studies have shown that, in addition to DAG-dependent recruitment (39, 40), PKC $\theta$  activation requires its localization to lipid rafts and is Lck-dependent but ZAP70-independent (36). Furthermore, Lck has been shown to coprecipitate with and directly phosphorylate PKC $\theta$  (37), and Lck-dependent phosphorylation of PKC $\theta$  enhances the membrane targeting and activation of PKC $\theta$  (41).

In LAT-Y136F CD4<sup>+</sup> T cells, we find enhanced basal association of Lck with PKC $\theta$  (Fig. 7A, 7B), which both enhanced the DAG-mediated membrane recruitment (Fig. 7C) and led to the activation of PKC $\theta$  (Fig. 7D). Furthermore, inhibition of SFK signaling reduced the activation of PKC $\theta$  (Fig. 8C). Once activated, PKC $\theta$  can directly phosphorylate and help activate RasGRP1. We observe elevated basal RasGRP1 phosphorylation on T184 (Fig. 7D) that was decreased by total but not typical PKC inhibition (Fig. 8C). These data suggest that the elevated PKC $\theta$  phosphorylation (Fig. 7D), downstream of SFK hyperactivation (Fig. 6B), activates RasGRP1/ERK signaling.

Studies using mutated, pathologic cells have led to the understanding of many fundamental signaling proteins, including Src (53–55) and Ras (56, 57), or novel signaling connections now recognized as important to normal cellular function (58). In T cells, much of our understanding of the molecular details of downstream TCR signaling comes from studying T cell leukemia cells and mutant animal models. Relevant to this study is that in addition to LAT-Y136F mutant mice, multiple animal models

carrying mutations in TCR- and/or IL-2-dependent signaling, including IL-2<sup>-/-</sup> (59), STAT5a/5b DKO (60), STIM1/2 DKO (61), NFATc2/c3 DKO (62), Vav1<sup>-/-</sup>Cbl-b<sup>-/-</sup> (63), and CD45-E613R mice (64), show a lymphoproliferative phenotype. Maintenance of proper signaling through these proteins and their downstream signaling targets likely represents an important physiological barrier to the development of lymphoproliferative disease.

When trying to understand the molecular mechanisms driving lymphoproliferation in LAT-Y136F mice, we noticed an unexpected ERK hyperactivation, and we have sought to explain both the origin and significance of ERK activation in these mice. Through the course of these studies, we have tested various mouse models known to signal to the ERK pathway, first describing a LAT-independent, Bam32-dependent pathway that accounts for some, but not all, of the ERK hyperactivation in LAT-Y136F mice (18). Based on these studies, we have recently defined a novel PLC- $\gamma$ 1/Bam32/PAK1 signaling pathway to ERK, which is independent of PLC- $\gamma$ 1 catalytic activity and functions under normal physiologic conditions (65). In this study, we describe how known, albeit less well understood, signaling connections can be rewired to produce pathologic RasGRP1-dependent Ras/ERK activation. These studies show that a tremendous amount of plasticity exists in TCR-dependent signaling, and that perturbation of canonical signaling pathways, although predicted to blunt signaling, may have unknown pathologic consequences. Understanding how the signaling environment is changed in these settings enhances our understanding of normal, alternative signaling pathways. Furthermore, these studies inform future targeted therapeutic choices by revealing both those signaling molecules that may represent good candidate targets and which perturbations might have unforeseen adverse consequences.

**Note added in proof.** After submission of this manuscript, a related article assessing the importance of the ERK pathway in lymphoproliferative disease in LAT-Y136F mice was published (66).

## Acknowledgments

We thank Lakshmi Balagopalan for helpful discussions throughout the project and for thoughtful reading of the manuscript. RasGRP1<sup>-/-</sup> mice were a gift from James Stone.

## Disclosures

The authors have no financial conflicts of interest.

## References

- Smith-Garvin, J. E., G. A. Koretzky, and M. S. Jordan. 2009. T cell activation. *Annu. Rev. Immunol.* 27: 591–619.
- Zhu, M., E. Janssen, and W. Zhang. 2003. Minimal requirement of tyrosine residues of linker for activation of T cells in TCR signaling and thymocyte development. *J. Immunol.* 170: 325–333.
- Balagopalan, L., N. P. Coussens, E. Sherman, L. E. Samelson, and C. L. Sommers. 2010. The LAT story: a tale of cooperativity, coordination, and choreography. *Cold Spring Harb. Perspect. Biol.* 2: a005512.
- Zhang, W., J. Sloan-Lancaster, J. Kitchen, R. P. Trible, and L. E. Samelson. 1998. LAT: the ZAP-70 tyrosine kinase substrate that links T cell receptor to cellular activation. *Cell* 92: 83–92.
- Zhang, W., R. P. Trible, M. Zhu, S. K. Liu, C. J. McGlade, and L. E. Samelson. 2000. Association of Grb2, Gads, and phospholipase C- $\gamma$ 1 with phosphorylated LAT tyrosine residues. Effect of LAT tyrosine mutations on T cell antigen receptor-mediated signaling. *J. Biol. Chem.* 275: 23355–23361.
- Roose, J. P., M. Mollenauer, V. A. Gupta, J. Stone, and A. Weiss. 2005. A diacylglycerol-protein kinase C-RasGRP1 pathway directs Ras activation upon antigen receptor stimulation of T cells. *Mol. Cell. Biol.* 25: 4426–4441.
- Margarit, S. M., H. Sondermann, B. E. Hall, B. Nagar, A. Hoelz, M. Pirruccello, D. Bar-Sagi, and J. Kuriyan. 2003. Structural evidence for feedback activation by Ras.GTP of the Ras-specific nucleotide exchange factor SOS. *Cell* 112: 685–695.

8. Das, J., M. Ho, J. Zikherman, C. Govern, M. Yang, A. Weiss, A. K. Chakraborty, and J. P. Roose. 2009. Digital signaling and hysteresis characterize ras activation in lymphoid cells. *Cell* 136: 337–351.
9. Roose, J. P., M. Mollenauer, M. Ho, T. Kurosaki, and A. Weiss. 2007. Unusual interplay of two types of Ras activators, RasGRP and SOS, establishes sensitive and robust Ras activation in lymphocytes. *Mol. Cell. Biol.* 27: 2732–2745.
10. Genot, E., and D. A. Cantrell. 2000. Ras regulation and function in lymphocytes. *Curr. Opin. Immunol.* 12: 289–294.
11. Kortum, R. L., C. L. Sommers, J. M. Pinski, C. P. Alexander, R. K. Merrill, W. Li, P. E. Love, and L. E. Samelson. 2012. Deconstructing Ras signaling in the thymus. *Mol. Cell. Biol.* 32: 2748–2759.
12. Zhang, W., C. L. Sommers, D. N. Burshtyn, C. C. Stebbins, J. B. DeJarnette, R. P. Tribble, A. Grinberg, H. C. Tsay, H. M. Jacobs, C. M. Kessler, et al. 1999. Essential role of LAT in T cell development. *Immunity* 10: 323–332.
13. Sommers, C. L., R. K. Menon, A. Grinberg, W. Zhang, L. E. Samelson, and P. E. Love. 2001. Knock-in mutation of the distal four tyrosines of linker for activation of T cells blocks murine T cell development. *J. Exp. Med.* 194: 135–142.
14. Aguado, E., S. Richelme, S. Nuñez-Cruz, A. Miazek, A. M. Mura, M. Richelme, X. J. Guo, D. Sainy, H. T. He, B. Malissen, and M. Malissen. 2002. Induction of T helper type 2 immunity by a point mutation in the LAT adaptor. *Science* 296: 2036–2040.
15. Nuñez-Cruz, S., E. Aguado, S. Richelme, B. Chetaille, A. M. Mura, M. Richelme, L. Pouyet, E. Jouvin-Marche, L. Xerri, B. Malissen, and M. Malissen. 2003. LAT regulates  $\gamma\delta$  T cell homeostasis and differentiation. *Nat. Immunol.* 4: 999–1008.
16. Sommers, C. L., C. S. Park, J. Lee, C. Feng, C. L. Fuller, A. Grinberg, J. A. Hildebrand, E. Lacaná, R. K. Menon, E. W. Shores, et al. 2002. A LAT mutation that inhibits T cell development yet induces lymphoproliferation. *Science* 296: 2040–2043.
17. Mingueneau, M., R. Roncagalli, C. Grégoire, A. Kissenpennig, A. Miazek, C. Archambaud, Y. Wang, P. Perrin, E. Bertosio, A. Sansoni, et al. 2009. Loss of the LAT adaptor converts antigen-responsive T cells into pathogenic effectors that function independently of the T cell receptor. *Immunity* 31: 197–208.
18. Miyaji, M., R. L. Kortum, R. Surana, W. Li, K. D. Woolard, R. M. Simpson, L. E. Samelson, and C. L. Sommers. 2009. Genetic evidence for the role of Erk activation in a lymphoproliferative disease of mice. *Proc. Natl. Acad. Sci. USA* 106: 14502–14507.
19. Dower, N. A., S. L. Stang, D. A. Bottorff, J. O. Ebinu, P. Dickie, H. L. Ostergaard, and J. C. Stone. 2000. RasGRP is essential for mouse thymocyte differentiation and TCR signaling. *Nat. Immunol.* 1: 317–321.
20. Esteban, L. M., A. Fernández-Medarde, E. López, K. Yienger, C. Guerrero, J. M. Ward, L. Tessarollo, and E. Santos. 2000. Ras-guanine nucleotide exchange factor sos2 is dispensable for mouse growth and development. *Mol. Cell. Biol.* 20: 6410–6413.
21. Lee, P. P., D. R. Fitzpatrick, C. Beard, H. K. Jessup, S. Lehar, K. W. Makar, M. Pérez-Melgosa, M. T. Sweetser, M. S. Schlissel, S. Nguyen, et al. 2001. A critical role for Dnmt1 and DNA methylation in T cell development, function, and survival. *Immunity* 15: 763–774.
22. Kortum, R. L., C. L. Sommers, C. P. Alexander, J. M. Pinski, W. Li, A. Grinberg, J. Lee, P. E. Love, and L. E. Samelson. 2011. Targeted Sos1 deletion reveals its critical role in early T-cell development. *Proc. Natl. Acad. Sci. USA* 108: 12407–12412.
23. Hanke, J. H., J. P. Gardner, R. L. Dow, P. S. Changelian, W. H. Brissette, E. J. Weringer, B. A. Pollok, and P. A. Connelly. 1996. Discovery of a novel, potent, and Src family-selective tyrosine kinase inhibitor: study of Lck- and FynT-dependent T cell activation. *J. Biol. Chem.* 271: 695–701.
24. Martiny-Baron, G., M. G. Kazanietz, H. Mischak, P. M. Blumberg, G. Kochs, H. Hug, D. Marmé, and L. Schächtele. 1993. Selective inhibition of protein kinase C isozymes by the indolocarbazole Gö 6976. *J. Biol. Chem.* 268: 9194–9197.
25. Toullec, D., P. Pianetti, H. Coste, P. Bellevergue, T. Grand-Perret, M. Ajakane, V. Baudet, P. Boissin, E. Boursier, F. Loriolle, et al. 1991. The bisindolylmaleimide GF 109203X is a potent and selective inhibitor of protein kinase C. *J. Biol. Chem.* 266: 15771–15781.
26. Gschwendt, M., H. J. Müller, K. Kielbassa, R. Zang, W. Kittstein, G. Rincke, and F. Marks. 1994. Rottlerin, a novel protein kinase inhibitor. *Biochem. Biophys. Res. Commun.* 199: 93–98.
27. Ebinu, J. O., S. L. Stang, C. Teixeira, D. A. Bottorff, J. Hooton, P. M. Blumberg, M. Barry, R. C. Bleakley, H. L. Ostergaard, and J. C. Stone. 2000. RasGRP links T-cell receptor signaling to Ras. *Blood* 95: 3199–3203.
28. Bleasdale, J. E., G. L. Bundy, S. Bunting, F. A. Fitzpatrick, R. M. Huff, F. F. Sun, and J. E. Pike. 1989. Inhibition of phospholipase C dependent processes by U-73, 122. *Adv. Prostaglandin Thromboxane Leukot. Res.* 19: 590–593.
29. Kim, J. G., I. Shin, K. S. Lee, and J. S. Han. 2001. D609-sensitive tyrosine phosphorylation is involved in Fas-mediated phospholipase D activation. *Exp. Mol. Med.* 33: 303–309.
30. Favata, M. F., K. Y. Horiuchi, E. J. Manos, A. J. Daulerio, D. A. Stradley, W. S. Feeser, D. E. Van Dyk, W. J. Pitts, R. A. Earl, F. Hobbs, et al. 1998. Identification of a novel inhibitor of mitogen-activated protein kinase kinase. *J. Biol. Chem.* 273: 18623–18632.
31. Castro, A. F., J. F. Rebhun, and L. A. Quilliam. 2005. Measuring Ras-family GTP levels in vivo: running hot and cold. *Methods* 37: 190–196.
32. Wange, R. L., R. Guitián, N. Isakov, J. D. Watts, R. Aebersold, and L. E. Samelson. 1995. Activating and inhibitory mutations in adjacent tyrosines in the kinase domain of ZAP-70. *J. Biol. Chem.* 270: 18730–18733.
33. Orloff, D. G., S. J. Frank, F. A. Robey, A. M. Weissman, and R. D. Klausner. 1989. Biochemical characterization of the  $\eta$  chain of the T-cell receptor: unique subunit related to  $\zeta$ . *J. Biol. Chem.* 264: 14812–14817.
34. Roy, S., A. Lane, J. Yan, R. McPherson, and J. F. Hancock. 1997. Activity of plasma membrane-recruited Raf-1 is regulated by Ras via the Raf zinc finger. *J. Biol. Chem.* 272: 20139–20145.
35. Mor, A., and M. R. Philips. 2006. Compartmentalized Ras/MAPK signaling. *Annu. Rev. Immunol.* 24: 771–800.
36. Bi, K., Y. Tanaka, N. Coudronniere, K. Sugie, S. Hong, M. J. van Stipdonk, and A. Altman. 2001. Antigen-induced translocation of PKC- $\theta$  to membrane rafts is required for T cell activation. *Nat. Immunol.* 2: 556–563.
37. Liu, Y., S. Witte, Y. C. Liu, M. Doyle, C. Elly, and A. Altman. 2000. Regulation of protein kinase C $\theta$  function during T cell activation by Lck-mediated tyrosine phosphorylation. *J. Biol. Chem.* 275: 3603–3609.
38. Kong, K. F., T. Yokosuka, A. J. Canonigo-Balancio, N. Isakov, T. Saito, and A. Altman. 2011. A motif in the V3 domain of the kinase PKC- $\theta$  determines its localization in the immunological synapse and functions in T cells via association with CD28. *Nat. Immunol.* 12: 1105–1112.
39. Carrasco, S., and I. Merida. 2004. Diacylglycerol-dependent binding recruits PKC $\theta$  and RasGRP1 C1 domains to specific subcellular localizations in living T lymphocytes. *Mol. Biol. Cell* 15: 2932–2942.
40. Díaz-Flores, E., M. Siliceo, C. Martínez-A, and I. Mérida. 2003. Membrane translocation of protein kinase C $\theta$  during T lymphocyte activation requires phospholipase C- $\gamma$ -generated diacylglycerol. *J. Biol. Chem.* 278: 29208–29215.
41. Melowic, H. R., R. V. Stahelin, N. R. Blatner, W. Tian, K. Hayashi, A. Altman, and W. Cho. 2007. Mechanism of diacylglycerol-induced membrane targeting and activation of protein kinase C $\theta$ . *J. Biol. Chem.* 282: 21467–21476.
42. Springael, C., S. Thomas, S. Rahmouni, A. Vandamme, M. Goldman, F. Willems, and O. Vosters. 2007. Rottlerin inhibits human T cell responses. *Biochem. Pharmacol.* 73: 515–525.
43. Sommers, C. L., J. Lee, K. L. Steiner, J. M. Gurson, C. L. Depersis, D. El-Khoury, C. L. Fuller, E. W. Shores, P. E. Love, and L. E. Samelson. 2005. Mutation of the phospholipase C- $\gamma$ 1-binding site of LAT affects both positive and negative thymocyte selection. *J. Exp. Med.* 201: 1125–1134.
44. Genton, C., Y. Wang, S. Izui, B. Malissen, G. Delsol, G. J. Fournié, M. Malissen, and H. Acha-Orbea. 2006. The Th2 lymphoproliferation developing in LatY136F mutant mice triggers polyclonal B cell activation and systemic autoimmunity. *J. Immunol.* 177: 2285–2293.
45. Schoenborn, J. R., Y. X. Tan, C. Zhang, K. M. Shokat, and A. Weiss. 2011. Feedback circuits monitor and adjust basal Lck-dependent events in T cell receptor signaling. *Sci. Signal.* 4: ra59.
46. Zikherman, J., C. Jenne, S. Watson, K. Doan, W. Raschke, C. C. Goodnow, and A. Weiss. 2010. CD45-Csk phosphatase-kinase titration uncouples basal and inducible T cell receptor signaling during thymic development. *Immunity* 32: 342–354.
47. Stefanová, I., B. Hemmer, M. Vergelli, R. Martin, W. E. Biddison, and R. N. Germain. 2003. TCR ligand discrimination is enforced by competing ERK positive and SHP-1 negative feedback pathways. *Nat. Immunol.* 4: 248–254.
48. Rao, N., S. Miyake, A. L. Reddi, P. Douillard, A. K. Ghosh, I. L. Dodge, P. Zhou, N. D. Fernandes, and H. Band. 2002. Negative regulation of Lck by Cbl ubiquitin ligase. *Proc. Natl. Acad. Sci. USA* 99: 3794–3799.
49. Liu, H., M. A. Purbhoo, D. M. Davis, and C. E. Rudd. 2010. SH2 domain containing leukocyte phosphoprotein of 76-kDa (SLP-76) feedback regulation of ZAP-70 microclustering. *Proc. Natl. Acad. Sci. USA* 107: 10166–10171.
50. Brockmeyer, C., W. Paster, D. Pepper, C. P. Tan, D. C. Trudgian, S. McGowan, G. Fu, N. R. Gascoigne, O. Acuto, and M. Salek. 2011. T cell receptor (TCR)-induced tyrosine phosphorylation dynamics identifies THEMIS as a new TCR signalosome component. *J. Biol. Chem.* 286: 7535–7547.
51. Malbec, O., M. Malissen, I. Isnardi, R. Lesourne, A. M. Mura, W. H. Fridman, B. Malissen, and M. Daëron. 2004. Linker for activation of T cells integrates positive and negative signaling in mast cells. *J. Immunol.* 173: 5086–5094.
52. Shan, X., R. Balakir, G. Criado, J. S. Wood, M. C. Seminario, J. Madrenas, and R. L. Wange. 2001. Zap-70-independent Ca<sup>2+</sup> mobilization and Erk activation in Jurkat T cells in response to T-cell antigen receptor ligation. *Mol. Cell. Biol.* 21: 7137–7149.
53. Brugge, J. S., and R. L. Erikson. 1977. Identification of a transformation-specific antigen induced by an avian sarcoma virus. *Nature* 269: 346–348.
54. Collett, M. S., J. S. Brugge, and R. L. Erikson. 1978. Characterization of a normal avian cell protein related to the avian sarcoma virus transforming gene product. *Cell* 15: 1363–1369.
55. Levinson, A. D., H. Oppermann, L. Levintow, H. E. Varmus, and J. M. Bishop. 1978. Evidence that the transforming gene of avian sarcoma virus encodes a protein kinase associated with a phosphoprotein. *Cell* 15: 561–572.
56. Langbeheim, H., T. Y. Shih, and E. M. Scolnick. 1980. Identification of a normal vertebrate cell protein related to the p21 src of Harvey murine sarcoma virus. *Virology* 106: 292–300.
57. Shih, T. Y., A. G. Papageorge, P. E. Stokes, M. O. Weeks, and E. M. Scolnick. 1980. Guanine nucleotide-binding and autophosphorylating activities associated with the p21src protein of Harvey murine sarcoma virus. *Nature* 287: 686–691.
58. Zimmermann, S., and K. Moelling. 1999. Phosphorylation and regulation of Raf by Akt (protein kinase B). *Science* 286: 1741–1744.
59. Gaffen, S. L., and K. D. Liu. 2004. Overview of interleukin-2 function, production and clinical applications. *Cytokine* 28: 109–123.
60. Snow, J. W., N. Abraham, M. C. Ma, B. G. Herndier, A. W. Pastuszak, and M. A. Goldsmith. 2003. Loss of tolerance and autoimmunity affecting multiple organs in STAT5A/5B-deficient mice. *J. Immunol.* 171: 5042–5050.
61. Oh-Hora, M., M. Yamashita, P. G. Hogan, S. Sharma, E. Lamperti, W. Chung, M. Prakriya, S. Feske, and A. Rao. 2008. Dual functions for the endoplasmic

- reticulum calcium sensors STIM1 and STIM2 in T cell activation and tolerance. *Nat. Immunol.* 9: 432–443.
62. Ranger, A. M., M. Oukka, J. Rengarajan, and L. H. Glimcher. 1998. Inhibitory function of two NFAT family members in lymphoid homeostasis and Th2 development. *Immunity* 9: 627–635.
63. Krawczyk, C., K. Bachmaier, T. Sasaki, R. G. Jones, S. B. Snapper, D. Bouchard, I. Koziarzki, P. S. Ohashi, F. W. Alt, and J. M. Penninger. 2000. Cbl-b is a negative regulator of receptor clustering and raft aggregation in T cells. *Immunity* 13: 463–473.
64. Majeti, R., Z. Xu, T. G. Parslow, J. L. Olson, D. I. Daikh, N. Killeen, and A. Weiss. 2000. An inactivating point mutation in the inhibitory wedge of CD45 causes lymphoproliferation and autoimmunity. *Cell* 103: 1059–1070.
65. Rouquette-Jazdanian, A. K., C. L. Sommers, R. L. Kortum, D. K. Morrison, and L. E. Samelson. 2012. LAT-independent Erk activation via Bam32-PLC- $\gamma$ 1-Pak1 complexes: GTPase-independent Pak1 activation. *Mol. Cell* 48: 298–312.
66. Fuller, D. M., M. Zhu, S. Koonpaew, M. I. Nelson, and W. Zhang. 2012. The importance of the Erk pathway in the development of linker for activation of T cells-mediated autoimmunity. *J. Immunol.* 189: 4005–4013.